PERGAMON

International Journal of Heat and Mass Transfer 45 (2002) 979–992

International Journal of HEAT and MASS TRANSFER

www.elsevier.com/locate/ijhmt

Heat transfer from an impinging premixed butane/air slot flame jet

L.L. Dong, C.S. Cheung, C.W. Leung *

Department of Mechanical Engineering, The Hong Kong Polytechnic University, Hung Hom, Kowloon, Hong Kong

Received 18 February 2001; received in revised form 30 June 2001

Abstract

Experiments were performed to study the heat transfer characteristics of a premixed butane/air slot flame jet impinging normally on a horizontal rectangular plate. The effects of Reynolds number and the nozzle-to-plate distance on heat transfer were examined. The Reynolds number varied from 800 to 1700, while the nozzle-to-plate distance ranged from $2d_e$ to $12d_e$. Comparisons were made between the heat transfer characteristics of slot jets and circular jets under the same experimental conditions. It was found that the slot flame jet produces more uniform heat flux profile and larger averaged heat fluxes than the circular flame jet. © 2002 Published by Elsevier Science Ltd.

Keywords: Premixed butane/air combustion; Flame impingement; Heat transfer; Slot jet

1. Introduction

Impinging jets have been of much interest because they are widely used in heating, cooling and drying processes to produce high heat and mass transfer rates. It has been recognized that nozzle geometry will have great influence on the operation of the impingement system [1]. Although the jets can be emitted from nozzles of any configuration, the most commonly used are axisymmetric circular and two-dimensional rectangular slot jets in practice, which are arranged either individually or in a multiple manner depending on the application [1–4]. Most of the investigations so far have concentrated on the circular jets. Furthermore, the studies on rectangular slot jets are mostly related to air jets [5]. Much less information about the impinging slot flame jet is available.

The previous work devoted to the impinging slot air jets has been carried out with experimental, numerical and analytical methods [6–17]. Huber [18] concluded that the hydrodynamics of an impinging slot jet is similar to that of the circular jet, with the major difference in the length of the potential core region. An isothermal slot jet has a potential core region with the length equal to 4.7–7.7 times the slot width, while an isothermal circular jet has a larger potential core region, which is equal to 6–7 times the nozzle diameters, according to Livingood and Hrycak [19]. Gutmark and Wolfshtein [20] investigated a slot air jet impinging normally on a plate and found that the jet was not affected by the presence of the plate over 75% of the entire vertical distance between the nozzle and the plate. Sezai and Mohamad [5] found the existence of pronounced streamwise velocity off-center peaks near the impingement plate from their numerical study of impinging laminar air jets, which were issuing from slots of different aspect ratios. Viskanta [21] suggested that the aerodynamics of a single flame jet was similar to that of the isothermal gas jet.

Gardon and Cobonpue [22] and Hollworth and Berry [23] found that slot nozzles were able to give even heat and mass transfer distributions. Wadsworth and Mudawar [24] found that a confined two-dimensional slot air jet might provide a larger impingement zone and ensure uniform coolant rejection following the impingement to offer possible benefits such as cooling effectiveness, uniformity and controllability. Hardisty [3] studied a variety of slot nozzles and found that narrower slots gave higher heat transfer coefficients for geomet-

* Corresponding author. Tel.: +852-2766-6651; fax: +852-2365-4703.

0017-9310/02/$ - see front matter © 2002 Published by Elsevier Science Ltd.
PII: S0017-9310(01)00215-0

Nomenclature

B	slot nozzle width (m)
C_P	specific heat of fluid (J/(kg K))
d_e	effective nozzle diameter (m)
h	total enthalpy per unit mass of gas (J/kg)
H	distance between the nozzle and the impingement plate (m)
L	slot nozzle length (m)
M	molecular weight (kg/mol)
Nu	Nusselt number ($=\alpha d/\lambda$)
$\dot{q}$	heat flux density (W/m^2)
r	radial distance from stagnation point (m)
Re	Reynolds number ($=u_{exit}d_e/v$)
T	temperature (K)
u	velocity of butane/air mixture (m/s)
Y	mole fraction

Greek symbols

α	heat transfer coefficient (W/m^2 K)
λ	thermal conductivity (W/m K)
v	kinematic viscosity (m^2/s)
μ	dynamic viscosity (kg/m s)
ρ	density (kg/m^3)
Ω	thermo-physical properties
ϕ	equivalence ratio (=(stoichiometric air/fuel volume ratio)/(actual air/fuel volume ratio))

Superscripts

$\sim$	weighted mean
–	averaged value

Subscripts

exit	at exit position
f	flame jet
i	mixture component including fuel and gas
mix	fuel/air mixture
p	impingement plate
s	stagnation point

rically similar arrangements. Sezai and Mohamad [5] observed two off-center peaks of the Nusselt number for air jets issuing from slot nozzles at a Reynolds number of 500. They concluded that the positions of the maximum Nusselt number corresponded to the positions of the off-center streamwise velocity peaks, which indicated that the off-center peaks of the Nusselt number were the result of the jet velocity profile near the impingement plate. Seyedein [25] investigated slot air jets discharging normally into a confined channel numerically and found that the highest Nusselt number occurred at the stagnation point due to the highest v-velocity gradient in the axial direction. Beyond the stagnation point the Nusselt number was decreased to an off-stagnation minimum, because of the growth of the laminar boundary layer as suggested by Polat [26]. Some distance beyond the off-stagnation minimum, the Nusselt number was increased to a secondary maximum. It was explained by Seyedein [25] as the result of the conversion of v-momentum to u-momentum in this region, which led to the increase of lateral velocity and consequently the heat transfer. However, Polat [26] attributed this phenomenon to the transition from laminar to turbulent flow.

Compared to the considerable investigations on impinging slot air jets, only very little work has been performed relating to the impinging slot flame jets. Most of the previous study on impinging flame jets concentrated on circular jets utilizing methane or natural gas [27–35]. Milson and Chigier [34] found that the dominant feature of both premixed and diffusion methane/air flames was the presence of a cool central core of unreacted gas. This caused the area of the plate around the stagnation point to be cooler than the location of maximum temperature, and the heat flux from the flame to the plate followed a similar pattern. Hargrave et al. [32] studied the impinging premixed methane/air flames and found that the peak heat flux occurred within or close to the flame reaction zone, because the mean velocity and temperature of the flame exhibited maxima in the vicinity of the reaction zone. Popiel et al. [35] investigated the impingement of a methane/air combustion product on a cold plate and found that, for large nozzle-to-plate distance, i.e., $H/d \geqslant 4$, the heat flux distribution along the radial distance was bell shaped. As the nozzle-to-plate distance was decreased below $H/d = 3.5$, the central maximum began to be replaced by a central minimum.

Schuller et al. [36] investigated impinging premixed methane/air and propane/air flame jets emitting from rectangular nozzle openings, which were used to simulate typical accidental flame jets emanating from rectangular cracks or flanges, with respect to the safety of offshore oil and gas production facilities. Their studies were only focused on the flame height, width and lift-off. There is a dearth in the literature concerning the heat transfer characteristics of an impinging slot flame jet, even though it is commonly used in commercial cooktops [37]. It is apparent that the design of gas-fired heat transfer equipment is therefore based largely on accumulated practical experience rather than scientific prediction and analysis.

The present work was carried out to study the heat transfer characteristics of an impinging slot flame jet firing LPG or butane gas, which is commonly used in domestic heating equipment. Experiments were per-

formed to investigate the influences of gas/air mixture Reynolds number at the nozzle exit and the nozzle-to-plate distance. The range of Reynolds number under consideration varied from 800 to 1700, which extended from a laminar flame to a transitional flame and was of practical interest in low-heat-value heating applications. The nozzle-to-plate spacing (H/d_e) ranged from 2 to 13, to include the potential core length of a slot jet. All the tests were performed at the stoichiometric condition, because it provides the most fuel efficient operation and is used in most heating processes [27]. Additional experiments were also carried out to compare the heat transfer characteristics between slot and circular flame jets under the same experimental conditions.

2. Experimental setup and method

The flame jet impingement system was composed of two parts: the heat generation system and the heat absorption system, as shown schematically in Fig. 1(a).

The flame holders of the heat generation system used in the present study had two cross-sectional shapes: one was a rectangular brass duct with an inner cross-section of 13.7 mm × 4.6 mm (the longer edge was placed along the x-axis as shown in Fig. 1(b)). The other was a circular brass duct with an inner diameter of 9 mm. The two ducts had the same length of 70 mm and the same cross-sectional areas. Metered butane and compressed air were premixed in a brass cylinder, before they were supplied to the cylindrical aluminum equalizing chamber

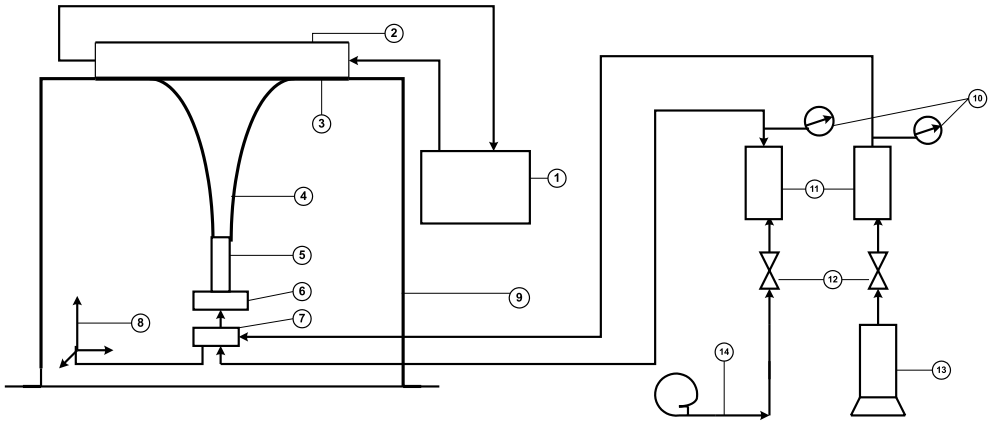

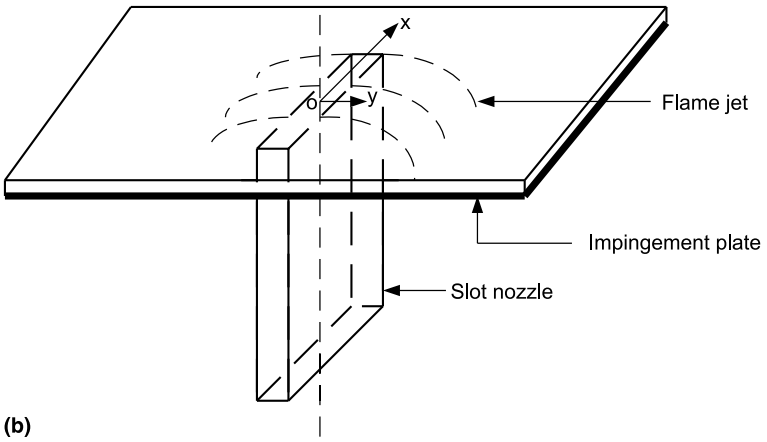

Fig. 1. (a) Schematic of the experimental setup; (b) coordinate system of the impingement plate.

via a 200 mm long stainless steel tube. The equalizing chamber was filled with stainless steel beads to equalize the flow and prevent the flame from flashing back. Then the mixture entered the flame holder and the flame ignited and stabilized at the rim. Both the inside surfaces of the flame holders were polished to even the exit velocity profile. The three-dimensional positioner enabled the attached burner to be fixed at a desired position relative to the impingement surface.

The flame impingement surface of the heat absorption system was a rectangular copper plate 200 mm long, 200 mm wide and 8 mm thick. Copper was selected because of its excellent thermal conductivity. It was evenly cooled on the reverse side by a cooling water jacket whose top plate was made of plexiglass to enable the water flow to be visible. A stainless steel frame was used to support the copper plate and the heat exchanger such that the plate could be placed either horizontally or tilted at a selected angle relative to the burner. The total heat transfer rate to the surface was determined calorimetrically by measuring the coolant's flow rate and its temperature change. After a change in the operating condition was made, measurements were only carried out when the steady state had been established again and exit temperature of the cooling water, which was measured with K-type thermocouples, had been stabilized.

The local heat flux from the flame to the plate was measured with a small ceramic heat flux transducer (Thermonetics) with a size of 3 mm × 3 mm × 0.8 mm. The calibrated accuracy was ±3%. It was attached directly to the copper plate near the pressure tap. Because it was very thin, its influence on the flow was negligible. Measurements of the radial heat flux distributions were carried out by moving the burner positioner horizontally.

The flame side surface temperatures of the impingement plate were measured with 14 T-type thermocouples. Each thermocouple was embedded in a small hole, which was drilled from the rear of the copper plate to within 1 mm of the impingement side. Two lines of holes were drilled at distances away from the plate center (i.e., $x = 0, y = 0$), with each line perpendicular to the other, and each thermocouple was spaced 15 mm apart from another. Flame temperatures were measured in the flame, against the location of each hole, with a bare wire B-type thermocouple. The measured flame temperatures were corrected for convection and radiation effects according to the method suggested by Bradley and Matthews [38]. A PC-Acquisitor was used to record the heat fluxes, the flame temperatures and the plate temperatures simultaneously.

Experiments were designed to identify, respectively, the influences of Reynolds number and nozzle-to-plate distance on the heat transfer characteristics of the impinging slot flame jet. Tests were first performed at five different nozzle exit Reynolds numbers of 800, 1000, 1200, 1500 and 1700, and constant equivalence ratio of 1 and $H/d = 6.0$. The influence of nozzle-to-plate distance was then investigated with values of H/d ranging from 2.0 to 13.0, at constant equivalence ratio of 1 and Reynolds number of 1700.

3. Calculation procedure and error analysis

The coordinate system used in the present study is shown in Fig. 1(b). The total heat flux, including convection and radiation, was measured with the heat flux transducer. It has been proposed by Popiel et al. [35] and Baukal and Gebhart [39] that radiation could be neglected because of the very low emissivity of non-luminous flame, which led to relatively low contribution of radiation to the total heat transfer from the flame to the plate. All the flames in the present study had the equivalence ratio of 1 and were non-luminous, with no soot deposition observed. The radiative heat flux was thus neglected in the present work.

To facilitate the handling of the data obtained from the slot nozzles, a characteristic dimension of the rectangular nozzle should be used. There were several choices existed according to Schuller et al. [36] including the slot width, the slot length, the slot hydraulic diameter and an effective diameter which produced the same exit momentum as that of the rectangular nozzle. The effective diameter was chosen in the present study for two reasons: first the jet length in general was a strong function of the jet exit momentum [36], second to facilitate and compare the data obtained from both slot and circular nozzles. The effective diameter of the nozzle is defined as

$$d_e = (4BL/\pi)^{1/2}. \tag{1}$$

The flame jet exit Reynolds number was evaluated based on cold fuel/air mixture gases as

$$Re = \frac{u_{exit} d_e \rho_{mix}}{\mu_{mix}}. \tag{2}$$

μ_{mix} was calculated according to Ikoku [40] as

$$\mu_{mix} = \frac{\sum(\mu_i Y_i \sqrt{M_i})}{\sum(Y_i \sqrt{M_i})}. \tag{3}$$

The boundary layer of an impinging flame jet is chemically reactive, where the gases are dissociated to atoms and radicals, and combined again exothermically when impinging on a cold plate to enhance the heat transfer. The enthalpy difference instead of the temperature difference between the flame and the plate has been identified as the driving force for total heat transfer. Considering the large temperature difference between the flame and the impingement plate, the thermo-phys-

ical properties applied in the present analysis were calculated based on the weighted average quantities instead of the film values, such as

$$\tilde{\Omega} = \frac{1}{T_f - T_p} \int_{T_p}^{T_f} \Omega(T)\,dT. \quad (4)$$

The local Nusselt number was then calculated from

$$Nu = \frac{\alpha d_e}{\lambda(\tilde{T})}. \quad (5)$$

From Newton's law of cooling, the heat transfer coefficient was expressed by

$$\alpha = \frac{\dot{q}}{T_f - T_p}. \quad (6)$$

Eqs. (5) and (6) were combined to give the definition of local Nusselt number, i.e.,

$$Nu = \frac{\dot{q} d_e}{\lambda(\tilde{T})(T_f - T_p)}. \quad (7)$$

It was assumed that the combustion products were perfect gases in calculating the enthalpy change, i.e.,

$$h_f - h_p = C_P|_0^{T_f} T_f - C_P|_0^{T_p} T_p = C_P|_{T_p}^{T_f}(T_f - T_p) = C_P(\tilde{T})(T_f - T_p). \quad (8)$$

Eq. (8) was substituted into Eq. (7) to provide

$$Nu = \frac{\dot{q} C_P(\tilde{T}) d_e}{(h_f - h_p)\lambda(\tilde{T})}, \quad (9)$$

where the values of $C_P(\tilde{T})$ and $\lambda(\tilde{T})$ were obtained from Eq. (4).

The uncertainty analysis was carried out using the method of Kline and McClintock [41]. The uncertainty in fuel equivalence ratio was 3.5%. The minimum and maximum uncertainties in the surface temperature measurements were 2.2% and 5.7%. The flame temperatures had minimum and maximum uncertainties of 2.7% and 8.9%, respectively. The minimum and maximum uncertainties in the surface heat flux profile were 4.7% and 14.2%, respectively.

To ensure repeatability of the results, three individual tests at identical operating conditions were performed and the data were then averaged. The maximum and minimum standard deviations of the local heat flux at the stagnation region were 15.5% and 1.8% of the mean value, whereas those of the near-plate flame temperature were 8.8% and 2.7%, respectively.

4. Results and discussions

Heat transfer results including the local and averaged heat fluxes were obtained under different Reynolds numbers and nozzle-to-plate distances, and they will be discussed in detail.

4.1. Local heat transfer distributions

4.1.1. Effects of Reynolds number

In the present study, the Reynolds numbers were selected to be 800, 1000, 1200, 1500 and 1700, at which the flame was extended from laminar to transitional conditions. All the flames under investigation showed the characteristics of a conical flame, which was stabilized at the rim of the burner nozzle. In the flame, a blue inner reaction zone with a nearly triangular cross-section and a light-blue outer layer were observed. The inner reaction zone had a sharp boundary between the unburnt and burnt gases. The outer layer impinged on the plate and then travelled radially along the plate, forming a conical flame as depicted by Zhang and Bray [42]. When the Reynolds number was less than 1500, the flame was everywhere laminar and formed a smooth sheet after it impinged on the plate. It then travelled radially outward, which agreed with the findings of Rigby and Webb [43]. When *Re* exceeded 1500, the inner reaction zone became shorter, thicker and more diffuse, which indicated the occurrence of transition from laminar to transitional flow conditions.

The three-dimensional plot of the heat flux distributions of a laminar flame, i.e., $Re = 1000$, and a transitional flame, i.e., $Re = 1700$, are shown in Fig. 2. It was apparent that, for the laminar flame, a cool central core with low heat flux occurred around the stagnation point, whereas the maximum heat flux occurred at some distance away from this point. It is clearly shown in Fig. 3 that when *Re* was less than 1500, the cool central core occurred. The location of maximum heat flux shifted gradually towards the stagnation point as the *Re* was increased. For a transitional flame, the maximum heat flux occurred at the stagnation point.

It was indicated in the present study that a cool central core was the feature of a laminar flame. For laminar flames, the inner reaction zone acted as a barrier against the progression of the fuel/air mixing process and prohibited the entrainment of the ambient air, which led to a direct impingement of the unreacted gas inside the inner reaction zone on the plate. The low temperature of the unreacted gas resulted in a low heat flux at the stagnation point. On the other hand, the occurrence of the maximum heat flux at the stagnation point for the transitional flames was due to two factors. Firstly, mixing of fuel and air was enhanced by the turbulence, which led to a more complete combustion. Secondly, according to Hargrave et al. [32], the maximum heat flux occurred within or close to the flame reaction zone because of the large concentration of reactive species there, which enhanced the convective heat transfer by diffusion and exothermic recombination in

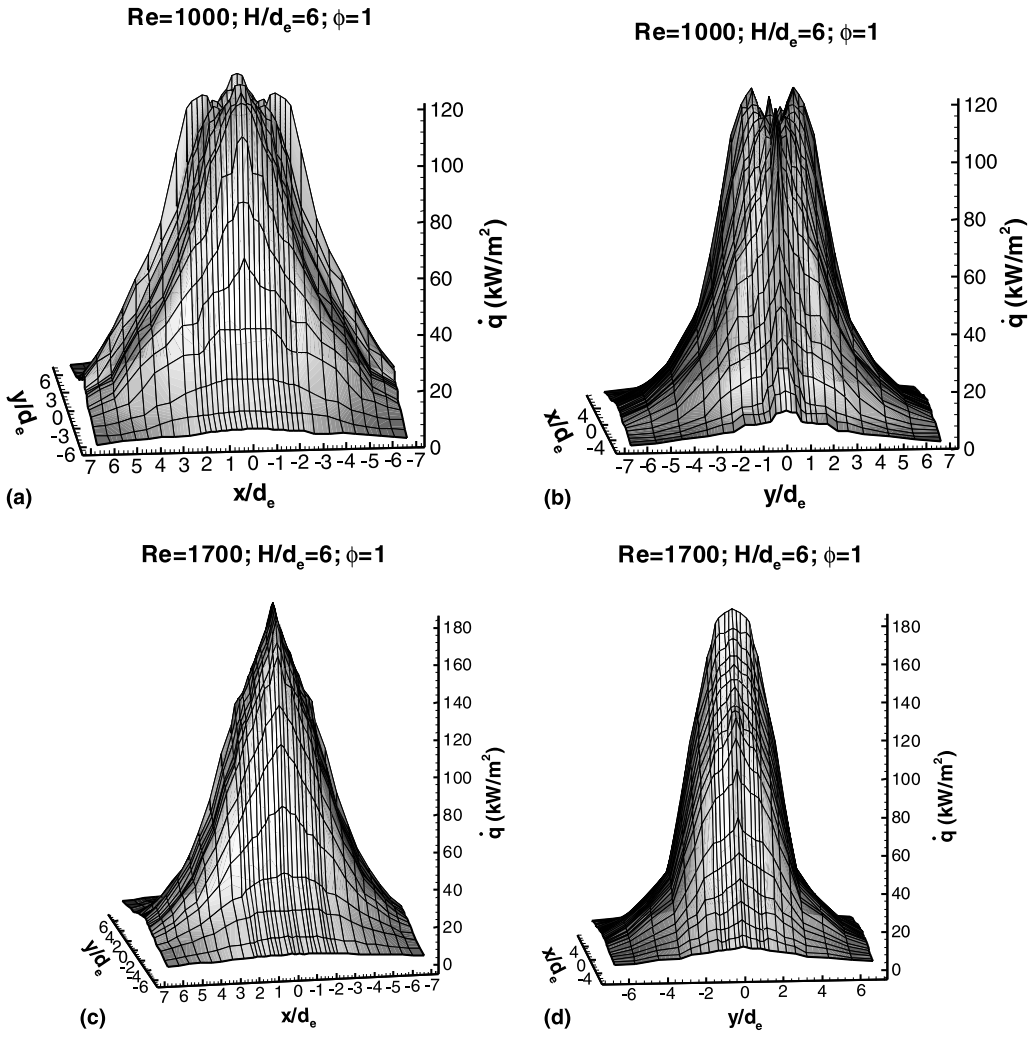

Fig. 2. Three-dimensional heat flux distribution.

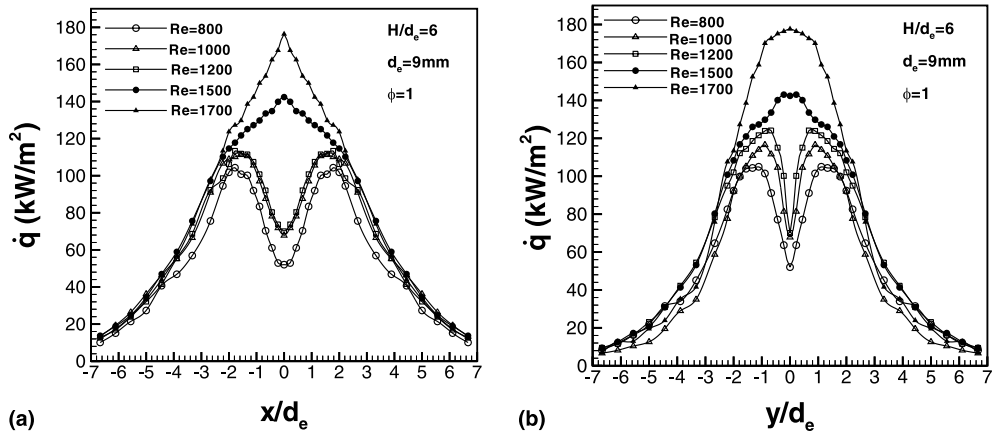

Fig. 3. Effect of *Re* on heat flux distribution.

the boundary layer surrounding the heat-receiving body. It could be concluded that the reaction zone, as well as the maximum heat flux, was shifting towards the stagnation point when the Reynolds number was increased from the laminar flow condition.

It is also observed from Figs. 2 and 3 that the influence of *Re* on heat transfer rate was more significant in the impingement and early wall jet regions. In the other regions, rather small differences were found between the heat flux distributions under different Reynolds numbers. It was because the heat flux was decreasing with the mean velocity and flow temperature downstream of the reaction zone.

It is obviously observed from Figs. 2 and 4 that the heat flux distributions in the x and y directions were rather different. In the impingement and early wall jet regions (i.e., when $r \leqslant 12$ mm for $Re = 1000$ or $r \leqslant 16$ mm for $Re = 1700$), the heat fluxes were higher along the y-axis than those along the x-axis. Beyond these points, the heat fluxes decayed faster along the y-axis than the x-axis. It might be due to the fact that the velocities in the y direction after impingement were higher than those in the x direction, which led to higher heat fluxes in the impingement and the early wall regions. In addition, the rectangular configuration of the nozzle allowed more fuel/air mixture to exit along its length rather than width, and thus the heat fluxes decayed slower in the x-axis than in the y-axis.

Fig. 5(a) shows the contour plot of the heat flux distribution on the impingement plate at *Re* of 1000, and a cool central area with relatively low heat fluxes is clearly observed. This was in accordance with Fig. 3. This was due to the direct impingement of the unreacted fuel/air mixture with low temperature on the plate. The

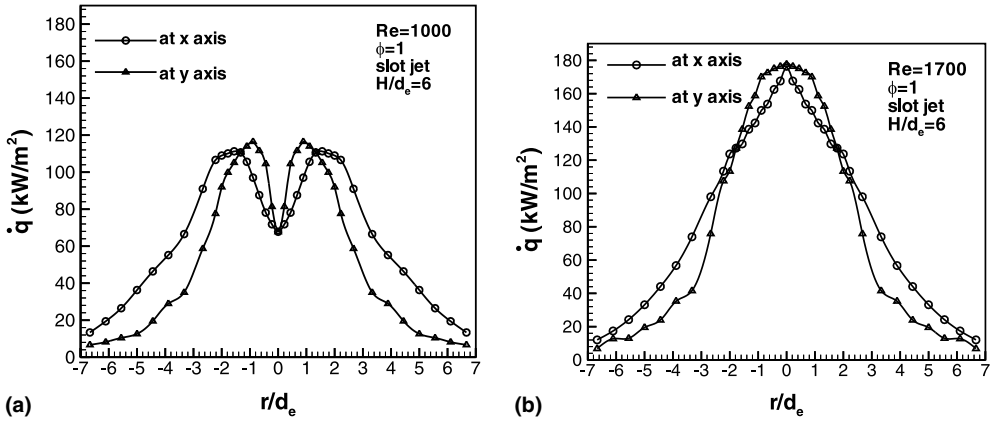

Fig. 4. Heat flux distribution along x and y axes.

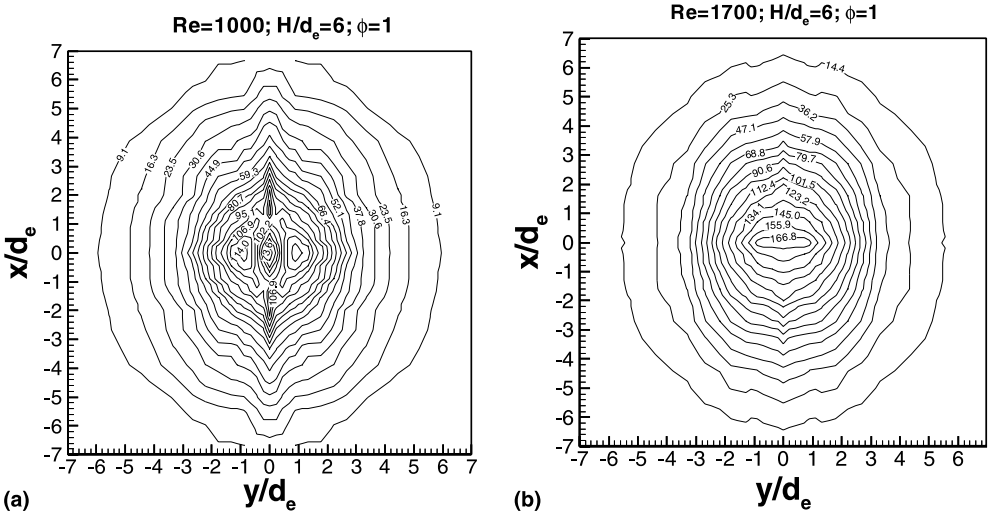

Fig. 5. Heat flux contours for $Re = 1000$ and $Re = 1700$.

heat flux increased gradually at positions moving away from the stagnation point in both the x and y axes and reached the maximum values, which was due to the occurrence of complete combustion in these positions. Beyond the locations of maximum heat flux, the heat fluxes decayed monotonically. The contour plot was of oval shape, and the heat flux gradient was greater in the y direction than that in the x direction, which implied that heat flux in the y direction increased faster in the impingement region and the early wall jet region and decayed faster in the other wall jet regions. A similar contour plot of heat flux distribution at Re of 1700 is shown in Fig. 5(b). It was observed that the heat flux decayed monotonically from the stagnation point. In the impingement and early wall regions, the heat flux gradient was higher in the x direction than that in the y direction, which implied that the heat flux decayed faster in the x direction in these regions. Beyond these regions, the heat flux gradient was higher in the y direction resulting in a contrary decaying trend.

The relationship between Reynolds number and the stagnation point Nusselt number is presented in Fig. 6(a). In the range of Re under consideration, i.e., $800 \leqslant Re \leqslant 1700$, Re and Nu_s had the following relation:

$$Nu_s = 0.56Re^{0.492}. \tag{10}$$

The proposed correlation is in good agreement with the theoretical solution of Sibulkin [44] for the heat transfer coefficient of the stagnation point formed by fluid flowing around a bluff body, where the exponent is found to be 0.5.

In practice, average rather than local values of the heat transfer rate are required. The average heat flux distribution for different Re is shown in Fig. 6(b). The average heat fluxes are obtained by integrating the local heat flux distributions with the trapezoid rule with three integration regions selected. One region is the impingement and early wall jet regions (i.e., $0 \leqslant r \leqslant 20$ mm), the second region is the other wall jet region (i.e., 20 mm $< r \leqslant 60$ mm), and the third region is the entire region under investigation (i.e., $0 \leqslant r \leqslant 60$ mm). The entire investigation region was split into two parts with the aim of providing a better identification of the high heat flux region occurring in the stagnation region and the early wall region, which was of higher practical value.

It is observed from Fig. 6(b) that the effect of Re on the average heat flux was different in different integration regions. In the impingement and early wall jet regions, there was an obvious increase in the average heat flux as the Re was increased. The average heat flux obtained by integrating over the entire investigation region increased with increasing Re, which is mainly due to the significant increase in the impingement and early wall jet regions. It is also observed in Fig. 6(b) that, in the impingement and early wall jet regions, the average heat fluxes were higher along the y-axis than those in the x-axis. In contrast, in the other wall jet regions, the average heat fluxes were higher along the x-axis, which led to a higher average heat flux at the x-axis than that at the y-axis for the entire region under investigation.

4.1.2. Effects of nozzle-to-plate distance

The effect of nozzle-to-plate distance (H/d_e) on the heat transfer characteristics of an impinging slot flame jet was investigated, with the values of H/d_e ranging from 2 to 13 to cover the potential core length. It was observed that H/d_e could affect the flame shape before impingement. When H/d_e was lower than 4, it was obviously observed that both the blue inner core and the light-blue outer layer impinged on and then travelled radially along the plate. When H/d_e exceeded 4, the brush-like inner reaction zone did not reach the plate, and the shape of the inner core exhibited a rectangle in the direction along the nozzle's length and a triangle in the direction along the nozzle's width. When H/d_e ex-

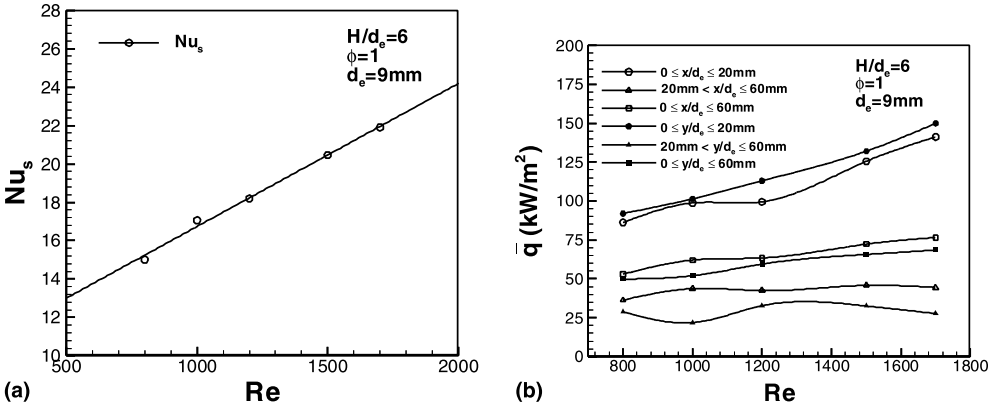

Fig. 6. Effect of Re on Nu_s and $\bar{q}$.

ceeded 7, the flame became unstable and started to flicker.

The three-dimensional heat flux distribution of the transitional flame under small nozzle-to-plate distance, i.e., $H/d_e = 3$, is shown in Fig. 7. It was observed that there was a cool central core. Fig. 8(a) also shows the existence of the cool central core when H/d_e was less than 4. It was because the reaction zone could not reach the axis of symmetry. The smaller the value of H/d_e, the more pronounced the cool central core was. When H/d_e reached 4, the maximum heat flux occurred at the stagnation point. When H/d_e was further increased, the stagnation point heat flux increased until the maximum value was reached at $H/d_e = 11$. It was the flickering of the flame at large nozzle-to-plate distance which increased the turbulence and thus the mixing of fuel and air. Further increase of H/d_e beyond this value led to a decrease of the stagnation point heat flux, because the nozzle-to-plate distance was larger than the flame length and the flame could not impinge on the plate.

Fig. 8(b) shows that the maximum heat flux occurred at the y-axis when $r < 8$ mm, and the heat fluxes along the y-axis were larger than those along the x-axis. Beyond this point a contrary trend existed. When 8 mm $\leqslant r < 28$ mm, the heat fluxes along the x-axis were larger than those along the y-axis. It could also be observed in Fig. 8(c), which was the contour plot for the flame at $Re = 1700$ and $H/d_e = 3$.

The relationship between the stagnation point Nusselt number and the nozzle-to-plate distance is shown in Fig. 9(a). Comparing Fig. 7 to Fig. 8(c) shows that the variation of the stagnation point heat transfer coefficient had the same trend as that of the stagnation point heat flux. When H/d_e was less than 5, there was an evident increase in Nu_s as H/d_e was increased. When $5 < H/d_e \leqslant 12$, there was only a slight increase of Nu_s when H/d_e was increased and the maximum Nusselt number was obtained at $H/d_e = 12$. For even larger H/d_e, Nu at the stagnation point began to decrease.

4.2. Average heat transfer distributions

The average heat flux distribution under different H/d_e is shown in Fig. 9(b). The selection of the integration region was the same to that in Fig. 6(b). It was observed that the maximum average heat fluxes in both the impingement region and the wall jet region were obtained when $H/d_e = 6$, resulting in the maximum average heat flux in the total investigation region occurring at $H/d_e = 6$. It could be explained in two aspects. One was due to the high heat fluxes in the impingement region around the stagnation point. The occurrence of the cool central core at small H/d_e reduced the average heat flux. The other was attributed to the use of an appropriate nozzle-to-plate distance, which enabled the outer layer of flame with high temperature to impinge on the plate and then travel along the plate towards the wall jet region, thus enhancing the heat transfer there. When H/d_e exceeded 7, the average heat flux decreased gradually as H/d_e was increased because the contact area between the flame and the plate reduced at high H/d_e.

4.3. Comparisons of heat transfer from slot and circular jets

With the aim of comparing the heat transfer characteristics between an impinging slot jet and a circular

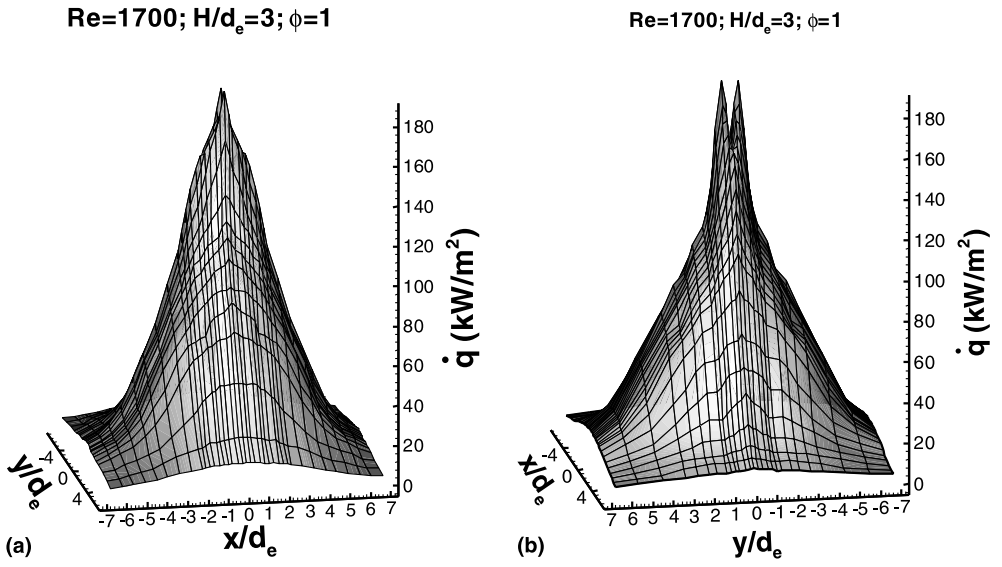

Fig. 7. Three-dimensional heat flux distribution.

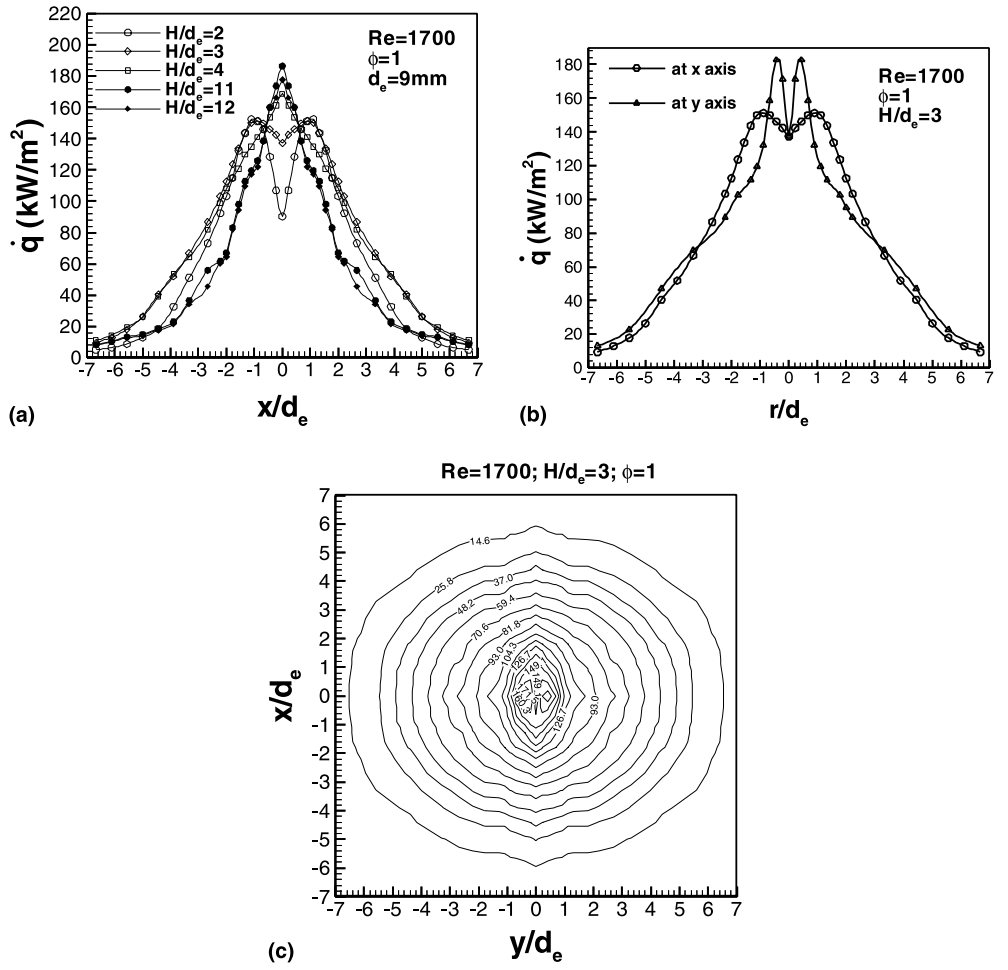

Fig. 8. (a) Effect of H/d_e on heat flux distribution; (b) heat flux distribution along x and y axes; (c) heat flux contour.

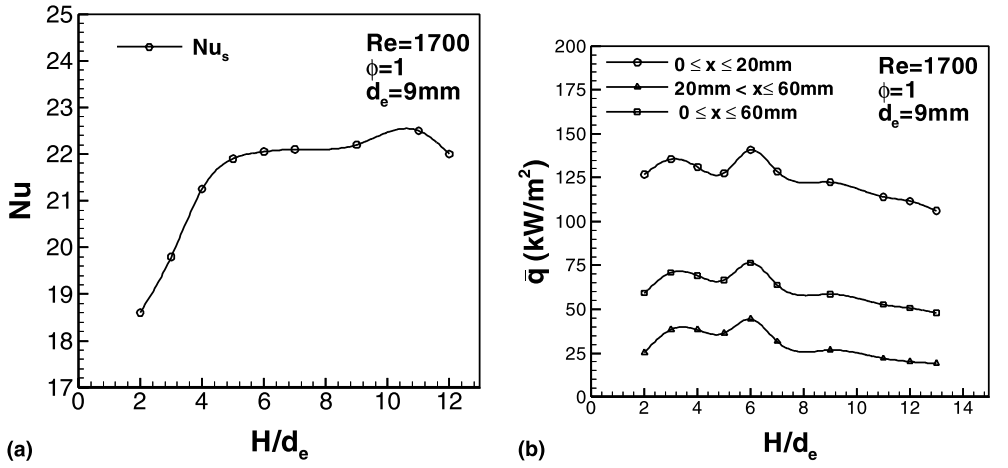

Fig. 9. Effect of H/d_e on Nu_s and $\bar{q}$.

jet, additional experiments were performed to study the thermal performance of circular jets under different Reynolds numbers with the other parameters remaining constant. The selected Reynolds numbers were the same as those for the slot jets, i.e., 800, 1000, 1200, 1500 and 1700. It was found that the flame emitting from a circular jet was conical in shape and was similar to that of the slot jets. The comparisons of heat flux distributions between the slot and the circular jets are shown in Fig. 10. It was found that for the laminar flames, i.e., $Re \leqslant 1200$, a cool central core with very low heat flux occurred in the flames for both the circular and slot jets. The heat fluxes at the stagnation point were lower in the circular flame jets than those in the slot flame jets, which indicated that the cool central core was more significant in the circular flame jets, i.e., in the region around the stagnation point, it was cooler in the circular jet flame than in the slot jet flame. With the same effective nozzle diameter, the width of a slot jet was much smaller than the diameter of a circular jet which facilitated the entrainment of ambient air into the region around the stagnation point to enhance the turbulence and hence the heat transfer in this area. Hardisty [3] found that narrower slots give higher heat transfer coefficients for the air jets. It was concluded from the present study that a narrower slot jet was able to produce higher heat transfer rate at the stagnation point for laminar flame jets. For the flame jets at $Re = 800$ and $Re = 1000$, the maximum heat fluxes for the circular jets were lower than those for the slot jets. However, such difference was reduced when the Re was increased to 1200, and became quite negligible when the Re was further increased to 1700. It was observed from Fig. 10(d) that the cool central core disappeared in the slot jet when the Re was increased to 1700, whereas it still existed in the circular jet. Fig. 10 also indicates that when the Re was increasing, the location of the maximum heat flux shifted towards the stagnation point gradually, and such inward shifting was faster for the slot jet than for the circular jet.

A comparison of the stagnation point Nusselt number was made between the slot jets and the circular jets as shown in Fig. 11. It was observed that Nu_s in the slot

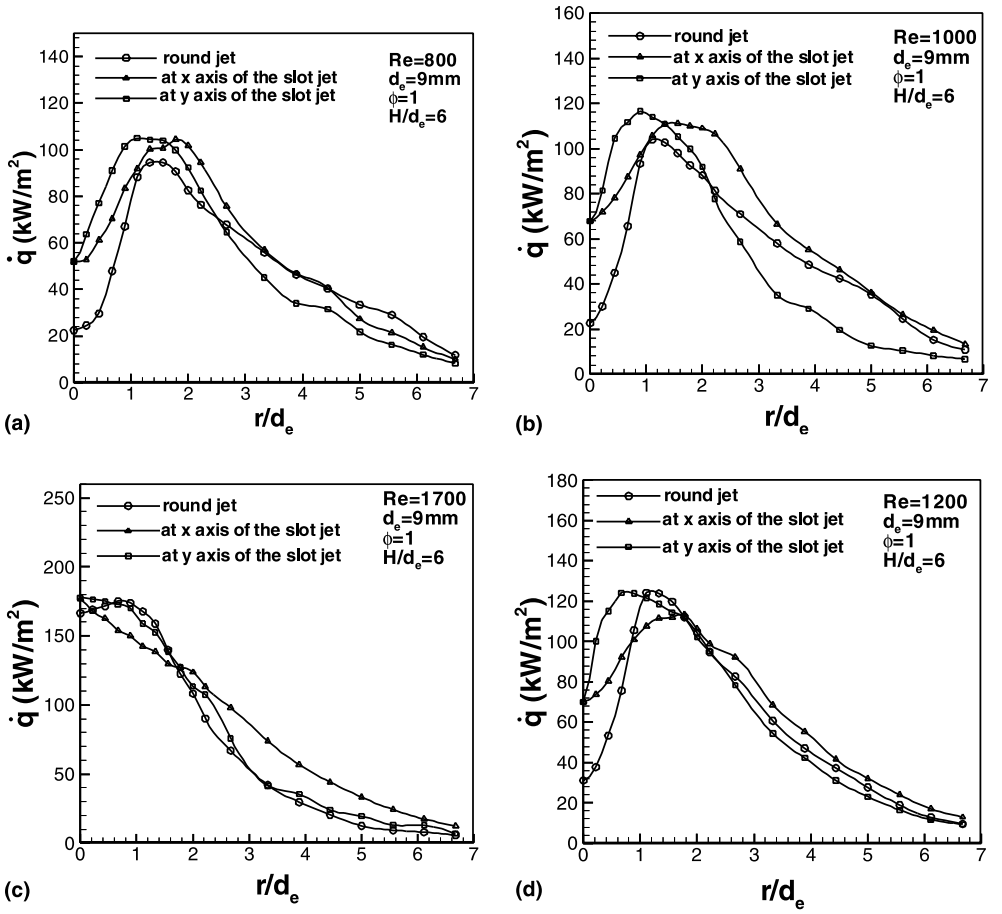

Fig. 10. Comparisons of the local heat fluxes between the circular and the slot jets under moderate nozzle-to-plate distance.

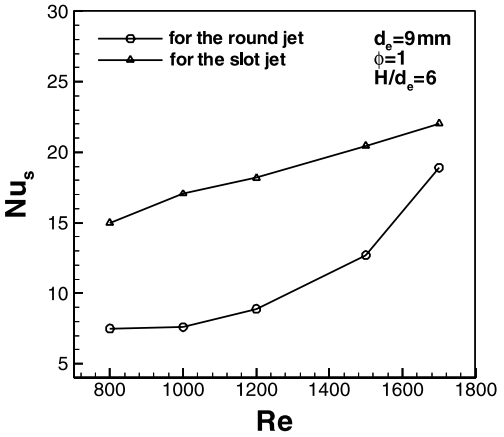

Fig. 11. Comparison of the stagnation point Nusselt number between the circular and the slot jets.

jets were larger than those in the circular jets within the investigation area. Such difference was rather significant for the laminar flames (i.e., $Re \leqslant 1200$) and became small for transitional flow (i.e., $Re = 1700$). In comparison with nozzle shape, this implied that turbulence has a greater effect on augmentation of heat transfer. This finding was in good agreement with that of Gardner [45], who found that the slot air jets yielded higher heat transfer coefficients than the circular air jets.

The comparison of average heat flux between the slot and circular flame jets is shown in Fig. 12. It was found that, for the laminar flames with $Re \leqslant 1200$, the average heat fluxes of the circular flame jet were lower than those of the slot flame jets along both the x and y axes. It was due to the existence of a larger cool central core in the circular flame jet as stated before. For the transitional flames, i.e., $Re \geqslant 1500$, the average heat fluxes of the circular flame jets were still lower than those along the x-axis, but became higher than those along the y-axis of the slot jets. The variations of the average heat fluxes with Re in the other wall jet regions are shown in Fig. 12(b). A contrary trend occurred in this region. It was observed that, for the laminar flames, values of the average heat flux of the circular flame jet were between those of the x and y axes of the slot jet. In addition, when the flame became transitional,

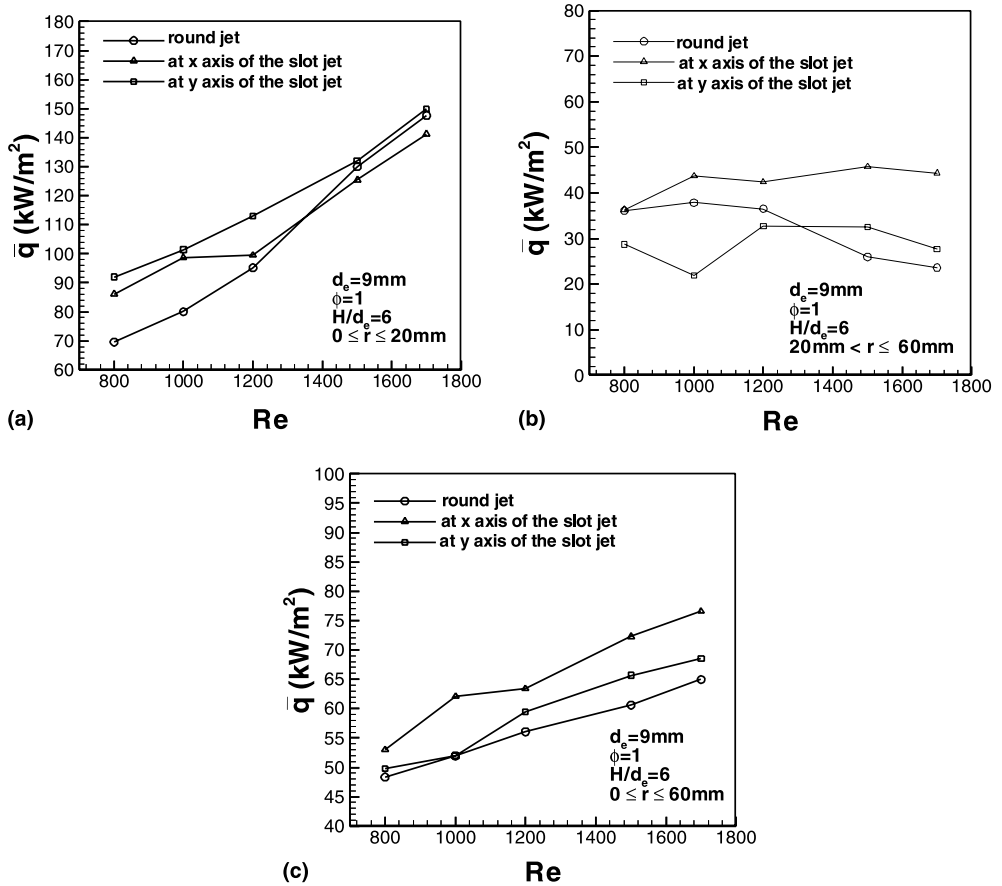

Fig. 12. Comparison of the average heat fluxes between the circular and the slot jets for different Re.

the average heat fluxes of the circular jet were the lowest. The comparison of the average heat fluxes between the slot and the circular flame jets for the entire investigation area is shown in Fig. 12(c). It was observed that the average heat fluxes of the circular flame jets were lower than those of the slot flame jets, with the highest values occurring at the x-axis of the slot jets.

5. Conclusions

Experiments were performed to study the heat transfer characteristics of a premixed butane/air flame slot jet impinging on a horizontal rectangular plate. Effects of Reynolds number and the nozzle-to-plate distance were examined. Both the local and average heat flux distributions were provided. Comparisons of heat transfer characteristics were made between slot jets and circular jets. The conclusions of the present study could be drawn as follows:

1. A cool central core of low heat flux values in the impinging flame occurred under two conditions: one was in the laminar flames (i.e., $Re < 1500$), and the other was at small nozzle-to-plate distances (i.e., $H/d_e < 4$). The cool central core became more evident when Re or H/d_e decreased.
2. For transitional flames (i.e., $Re > 1500$) under a moderate nozzle-to-plate distance (i.e., $H/d_e \geqslant 4$), the maximum heat flux occurred at the stagnation point.
3. The heat flux distributions were different at the x-axis and the y-axis. With the use of a moderate nozzle-to-plate distance, the heat flux gradients at the x-axis were always larger than those at the y-axis for both laminar and transitional flames.
4. The effect of enhancing heat transfer of Re was mainly exhibited in the impingement and early wall jet regions (i.e., $r \leqslant 20$ mm). In contrast, Re had little influence in the heat transfer in the other wall jet regions.
5. The average heat flux at the x-axis was larger than that at the y-axis due to the effect of the nozzle configuration (i.e., the longer edge of the rectangular nozzle was placed along the x-axis).
6. The maximum average heat flux occurred at a moderate nozzle-to-plate distance, i.e., $H/d_e = 6$.
7. The effect of the cool central core was more pronounced in the circular flame jets than in the slot flame jets due to influence of the nozzle shape. This led to the stagnation point heat flux being lower in the circular jet than that in the slot jet, as well as to a slower inwards shifting of the location of the maximum heat flux in the circular jets than in the slot jets.
8. A large heat flux enhancement at the stagnation point was obtained to be about two times (i.e., from 70 to 142 kW/m^2) when Re was increased from 1200 to 1500. The maximum heat flux obtained in the slot flame jet was found to be larger than that in the round flame jet when $Re < 1200$, while reaching almost the same value when $Re > 1200$.
9. For the laminar flame jets (i.e., $Re \leqslant 1200$), the average heat fluxes were larger in the slot jets than those in the circular jets in the impingement and the early wall jet regions. In the other wall jet regions, the average heat fluxes in the circular jets located between those in the x and y axes of the slot jets. The average heat fluxes were found to be larger in the slot jets than those in the circular jets in the entire investigation area.

Acknowledgements

The authors wish to thank The Hong Kong Polytechnic University for the financial support of the present study. The project code is GV-323.

References

[1] A.S. Mujumdar, Impingement drying, in: A.S. Mujumdar (Ed.), Handbook of Industrial Drying, McGill University, 1987, pp. 461–474.
[2] T. Cziesla, E. Tandogan, N.K. Mitra, Large-eddy simulation of heat transfer from impinging slot jets, Numer. Heat Transfer Part A 32 (1997) 1–17.
[3] H. Hardisty, An experimental investigation into the effect of changes in the geometry of a slot nozzle on the heat transfer characteristics of an impinging air jet, Proc. Inst. Mech. Eng. C 197 (1984) 7–15.
[4] N.R. Saad, S. Polat, J.M. Douglas, Confined multiple impinging slot jets without crossflow effects, Int. J. Heat Fluid Flow 13 (1992) 2–14.
[5] I. Sezai, A.A. Mohamad, Three-dimensional simulation of laminar rectangular impinging jets, flow structure, and heat transfer, J. Heat Transfer 121 (1999) 50–56.
[6] H. Miyazaki, E. Silberman, Flow and heat transfer on a flat plate normal to a two-dimensional laminar jet issuing from a nozzle of finite height, Int. J. Heat Mass Transfer 15 (1972) 2097–2107.
[7] T. Pekdemir, T.W. Davies, Mass transfer from rotating circular cylinders in a submerged slot jet of air, Int. J. Heat Mass Transfer 41 (1998) 3441–3450.
[8] Y.K., Chong, Two-dimensional slot jet impingement in a confined cross-flow stream, M.Sc. Thesis, Cranfield Institute of Technology, 1979.
[9] M. Korger, F. Křížek, Mass-transfer coefficient in impingement flow from slotted nozzles, Int. J. Heat Mass Transfer 9 (1966) 337–344.
[10] A.R.P. van Heiningen, A.S. Mujumdar, W.J.M. Douglas, Numerical prediction of the flow field and impingement heat transfer caused by a laminar slot jet, J. Heat Transfer 98 (1976) 654–658.
[11] E.M. Sparrow, T.C. Wong, Impingement transfer coefficients due to initially laminar slot jets, Int. J. Heat Mass Transfer 18 (1975) 597–605.

[12] S. Mikhail, S.M. Morcos, M.M.M. Abou-Ellail, W.S. Ghaly, Numerical prediction of flow field and heat transfer from a row of laminar slot jets impinging on a flat plate, Heat Transfer (3) (1982) 377–382.
[13] E.M. Sparrow, L. Lee, Analysis of flow field and impingement heat/mass transfer due to a nonuniform slot jet, J. Heat Transfer 97 (1975) 191–197.
[14] S.H. Seyedein, M. Hasan, A.S. Mujumdar, Laminar flow and heat transfer from multiple impinging slot jets with an inclined confinement surface, Int. J. Heat Mass Transfer 37 (1993) 1867–1875.
[15] S.H. Seyedein, M. Hasan, A.S. Mujumdar, Modelling of a single confined turbulent slot jet impingement using various κ–ϵ turbulence models, Appl. Math. Model. 18 (1994) 526–537.
[16] A.H. Beitelmal, M.A. Saad, C.D. Patel, The effect of inclination on the heat transfer between a flat surface and an impinging two-dimensional air jet, Int. J. Heat Fluid Flow 21 (2000) 156–163.
[17] S. Ashforth-Frost, K. Jambunathan, C.F. Whitney, Velocity and trubulence characteristics of a semiconfined orthogonally impinging slot jet, Exp. Therm. Fluid Sci. 14 (1997) 60–67.
[18] A. M. Huber, Heat transfer with impinging gaseous jet systems, Ph.D. Thesis, Purdue University, 1993.
[19] J.N.B. Livingood, P. Hrycak, Impingement heat transfer from turbulent air jets to flat plates – a literature survey, NASA TM X-2778, 1973.
[20] E. Gutmark, M. Wolfshtein, The plane turbulent impinging jet, J. Fluid Mech. 88 (1978) 737–756.
[21] R. Viskanta, Heat transfer to impinging isothermal gas and flame jets, Exp. Therm. Fluid Sci. 6 (1993) 111–134.
[22] R. Gardon, J. Cobonpue, Heat transfer between a flat plate and jets of air impinging on it, Int. Dev. Heat Transfer Part 2 (1961).
[23] B.R. Hollworth, R.D. Berry, Heat transfer from arrays of impinging jets with large jet-to-jet spacing, ASME 78-GT-117, 1978.
[24] D.C. Wadsworth, I. Mudawar, Cooling of a multichip electronic module by means of confined two-dimensional jets of dielectric liquid, J. Heat Transfer 112 (1990) 891–898.
[25] S.H. Seyedein, Simulation of fluid flow and heat transfer in impingement flows of various configurations, M.Sc. Thesis, McGill University, 1993.
[26] S. Polat, Transport phenomena under jets impinging on a moving surface with throughflow, Ph.D. Thesis, McGill University, 1988.
[27] C.E. Baukal, Heat transfer from flame impingement normal to a plane surface, Ph.D. Thesis, University of Pennsylvania, 1996.
[28] E. Buhr, G. Haupt, H. Kremer, Heat transfer from impinging turbulent jet flames to plane surfaces, in: Combustion Institute European Symposium, 1973, pp. 607–612.
[29] M. Fairweather, J.K. Kilham, Mohebi-Ashtiani, Stagnation point heat transfer from turbulent methane–air flames, Combust. Sci. Technol. 35 (1984) 225–238.
[30] M. Fairweather, J.K. Kilham, S. Nawaz, Stagnation point heat transfer from laminar, high temperature methane flames, Int. J. Heat Fluid Flow 5 (1984) 21–27.
[31] G.K. Hargrave, M. Fairweather, J.K. Kilham, Forced convective heat transfer from premixed flames – Part 1: flame structure, Int. J. Heat Fluid Flow 8 (1987) 55–63.
[32] G.K. Hargrave, M. Fairweather, J.K. Kilham, Forced convective heat transfer from premixed flames, Int. J. Heat Fluid Flow 8 (1987) 132–138.
[33] K. Kataoka, H. Shundoh, H. Matsuo, Convective heat transfer between a flat plate and a jet of hot gas impinging on it, in: Drying'84, 1984, pp. 218–227.
[34] A. Milson, N.A. Chigier, Studies of methane and methane–air flames impinging on a cold plate, Combust. Flame 21 (1973) 295–305.
[35] Cz.O. Popiel, Th.H. van der Meer, C.J. Hoogendoorn, Convective heat transfer on a plate in an impinging circular hot gas jet of low Reynolds number, Int. J. Heat Mass Transfer 23 (1980) 1055–1068.
[36] R.B. Schuller, J. Nylund, O.K. Sønju, J. Hustad, Effect of nozzle geometry on burning subsonic hydrocarbon jets, Fire Dyn. Heat Transfer 25 (1983) 33–36.
[37] R. Junus, J.F. Stubington, G.D. Sergeant, The effects of design factors on emissions from natural gas cooktop burners, Int. J. Env. Stud. 45 (1994) 101–121.
[38] D. Bradley, K.J. Matthews, Measurement of high gas temperatures with fine wire thermocouples, J. Mech. Eng. Sci. 10 (1968) 299–305.
[39] C.E. Baukal, B. Gebhart, Surface condition effects on flame impingement heat transfer, Exp. Therm. Fluid Sci. 15 (1997) 323–335.
[40] C.U. Ikoku, Natural Gas Production Engineering, 1984, pp. 58–60.
[41] S.J. Kline, F.A. McClintock, Describing uncertainties in single sample experiments, Mech. Eng. 75 (1953) 3–8.
[42] Y. Zhang, K.N.C. Bray, Characterization of impinging jet flames, Combust. Flame 116 (1999) 671–674.
[43] J.R. Rigby, B.W. Webb, An experimental investigation of diffusion flame jet impingement heat transfer, in: ASME/JSME Thermal Engineering Conference, vol. 3, 1995, pp. 117–126.
[44] M. Sibulkin, Heat transfer near the forward stagnation point at a body of revolution, J. Aeronaut. Sci. 19 (1952) 570–571.
[45] T.A. Gardner, A theory of drying with air, in: Tappi 43, 1960, pp. 796–800.